# Automated Search for new Quantum Experiments

Mario Krenn,[1,2,*] Mehul Malik,[1,2] Robert Fickler,[1,2,†] Radek Lapkiewicz,[1,2,‡] and Anton Zeilinger[1,2]
[1]Vienna Center for Quantum Science and Technology (VCQ), Faculty of Physics, University of Vienna, Boltzmanngasse 5, A-1090 Vienna, Austria
[2]Institute for Quantum Optics and Quantum Information (IQOQI), Austrian Academy of Sciences, Boltzmanngasse 3, A-1090 Vienna, Austria
(Received 30 September 2015; published 4 March 2016)

Quantum mechanics predicts a number of, at first sight, counterintuitive phenomena. It therefore remains a question whether our intuition is the best way to find new experiments. Here, we report the development of the computer algorithm MELVIN which is able to find new experimental implementations for the creation and manipulation of complex quantum states. Indeed, the discovered experiments extensively use unfamiliar and asymmetric techniques which are challenging to understand intuitively. The results range from the first implementation of a high-dimensional Greenberger-Horne-Zeilinger state, to a vast variety of experiments for asymmetrically entangled quantum states—a feature that can only exist when both the number of involved parties and dimensions is larger than 2. Additionally, new types of high-dimensional transformations are found that perform cyclic operations. MELVIN autonomously learns from solutions for simpler systems, which significantly speeds up the discovery rate of more complex experiments. The ability to automate the design of a quantum experiment can be applied to many quantum systems and allows the physical realization of quantum states previously thought of only on paper.

DOI: 10.1103/PhysRevLett.116.090405

Quantum mechanics encompasses a wide range of counterintuitive phenomena such as teleportation [1,2], quantum interference [3], quantum erasure [4], and entanglement [5–10]. Despite our struggle to reconcile them with our picture of reality, these phenomena serve as building blocks for many exciting and useful quantum technologies such as quantum cryptography [11,12], computation [13,14], and metrology [15,16]. A significant challenge arises, however, when we try to combine such phenomena in order to perform a complex quantum task. Understanding the outcome of even a simple combination of these quantum building blocks can be daunting for the human intuition. Therefore, it is natural to ask: Given a certain desired property of a quantum system, what combination of quantum building blocks will be successful in achieving it?

In order to answer this question, we develop a classical computer algorithm called MELVIN, to which we teach how these quantum phenomena work and, subsequently, assign it a specific problem. The machine then takes on the task of finding and optimizing arrangements of quantum building blocks that result in a solution. This allows us to uncover experimental methods to create an array of new types of entangled states previously thought to exist only in theory. In addition, it also allows us to address the question of how to manipulate such high-dimensional quantum states, which is key for their use in quantum information systems.

While searching for these experiments, MELVIN enlarges its own toolbox by identifying useful groups of elements, leading to a significant speed-up in subsequent discoveries. The experiments found by our algorithm show a departure from conventional experiments in quantum mechanics in that they rely on highly unfamiliar, but perfectly conceivable experimental techniques. This provides some insight into the kind of out-of-the-box thinking that is required for creating such complex quantum states.

Our method aims to create and manipulate general complex quantum states for which arbitrary transformations are not known. The algorithm creates experiments using experimentally accessible optical components that can readily be implemented in the laboratory [17,18]. In addition, our algorithm considers multiple degrees of freedom of single quantum systems and can be extended to include nonlinear components and states more complex than single photons. This would allow us to investigate many other interesting quantum phenomena such as NOON states [19], induced coherence [20,21], quantum teleportation of more complex systems [2], or quantum metrology [15,16]. A complementary field is computer assisted or automated quantum circuit synthesis (QCS) [22–26], where optimal implementations for quantum algorithms are designed from universal sets of known quantum gates. While very powerful in its own right, the technique of QCS is used for linear qubit networks and usually requires fault-tolerant quantum computers for the implementation of its results.

*The algorithm.*—The main goal is to develop an algorithm which finds experimental implementations for quantum states or quantum transformations with interesting properties, see Fig. 1. Specific possible input states and a toolbox of experimentally known transformations utilizable by MELVIN are defined initially. Using the elements from the toolbox, the algorithm assembles new experiments by arranging elements randomly. Then, from the initial state,

 

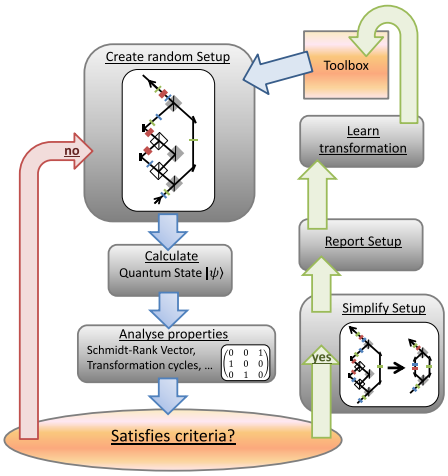


FIG. 1. Working principle of the algorithm. First, an experiment is created using elements from a basic toolbox. Then, the quantum state is calculated, and subsequently, its properties are analyzed. Those properties are compared with a number of criteria. If these criteria are not satisfied, the algorithm starts over again. However, if the criteria are satisfied, the experiment is simplified and reported, together with all relevant information for the user. Useful solutions can be stored and used in future experiments, which significantly increases the discovery rate of more complex experiments. The orange boxes (toolbox and criteria) are adapted when a different type of quantum property is investigated, while the rest of the algorithm stays the same.

the resulting quantum state and transformation is calculated, and its properties are analyzed. Well-defined criteria that are provided by the user decide whether the calculated quantum state has the desired properties. If the quantum state's properties satisfy the criteria, the experimental configuration is simplified and reported to the user. MELVIN can store the configuration in order to use it as a basic building element in subsequent trials. By extending the initial toolbox, it is learning from experience, which leads to a significant speed-up in discoveries of more complex solutions.

All quantum states are calculated using symbolic algebra. Every experimental element is a symbolic modification of the input state. As an example, a 50/50 symmetric non-polarizing beam splitter (BS) for photons is described by

$$\mathrm{BS}[\psi,a,b]=\psi\Leftarrow\begin{cases}a[\ell]\rightarrow\frac{1}{\sqrt{2}}(b[\ell]+ia[-\ell])\\ b[\ell]\rightarrow\frac{1}{\sqrt{2}}(a[\ell]+ib[-\ell])\end{cases},\quad(1)$$

where $\Leftarrow$ stands for a symbolic replacement followed by a list of substitution rules. $\ell$ stands for the orbital angular momentum (OAM) quantum number of the photon, and $a$ and $b$ denote the input paths of the beam splitter. For simplicity, all other degrees of freedom (such as polarization or frequency) are considered to be the same for all photons. For example, for the two-photon state $\psi=a[3]b[-3]$ ($a$ and $b$ represent the path of one photon, $+3$ and $-3$ stand for the OAM of the photon), the beam splitter in path $a$ and $b$ will lead to photon bunching, $\mathrm{BS}[\psi,a,b]\rightarrow(a[-3]^2+b[3]^2)$, which is the well-known Hong-Ou-Mandel effect [3]. By realizing the calculations with symbolic algebra, adding new elements or even new degrees of freedom is very easy [27]. Furthermore, it allows easy human-readable intermediate forms, important for the examination of solutions and the novel techniques found by the algorithm.

Next, we demonstrate the working principles using two concrete examples. The demonstrations work in the regime of photonic quantum experiments, but the algorithm can readily be adapted to (a combination of) other systems such as cold atoms [28].

*Example 1: High-dimensional multipartite entanglement.*—The Greenberger-Horne-Zeilinger (GHZ) state is the most prominent example of nonclassical correlations between more than two involved parties and has led to new understanding of the fundamental properties of quantum physics [8]. It has been shown recently that its generalization to higher dimensions not only has curious properties [10], but that it is a limiting case of a much richer class of nonclassical correlations [9,29,30]. These new structures of multipartite high-dimensional entanglement are characterized by the Schmidt-rank vector and give rise to new phenomena that only exist if both the number of particles and the number of dimensions are larger than two. An example of a state with Schmidt-rank vector (4,2,2) is the asymmetrically entangled state $|\psi_{4,2,2}\rangle=\frac{1}{2}(|0,0,0\rangle+|1,0,1\rangle+|2,1,0\rangle+|3,1,1\rangle)$. Here, the first particle is four-dimensionally entangled with the other two parties, whereas particle two and three are both only two-dimensionally entangled with the rest. This master-slave-slave configuration is one of the yet unexplored features that only exist in genuine high-dimensional multipartite entanglement and will be interesting to study in more detail in future. In order to make future experimental investigations possible, we aim to find high-dimensional multipartite entangled states in photonic systems.

Here, the initial state is created by a double spontaneous parametric down-conversion (SPDC) process. SPDC is a widespread source for the experimental generation of photon pairs. Multiple SPDC processes can be used to produce multipartite entanglement, as it is well known for the case of two-dimensional polarization entanglement [31,32]. However, instead of polarization, we use the OAM of photons [33–36], which is a discrete high-dimensional degree of freedom based on the spatial structure of the photonic wave function.

The experiments are generated using a set of basic elements consisting of beam splitters, mirrors, Dove prism, holograms, and OAM-parity sorters [27,37]. The holograms and the Dove prisms have discrete parameters corresponding to the OAM and phase added to the beam, respectively. These elements are randomly placed in one out of six different paths (four of the paths are inputs of the two photon pairs and two are empty to increase variability).

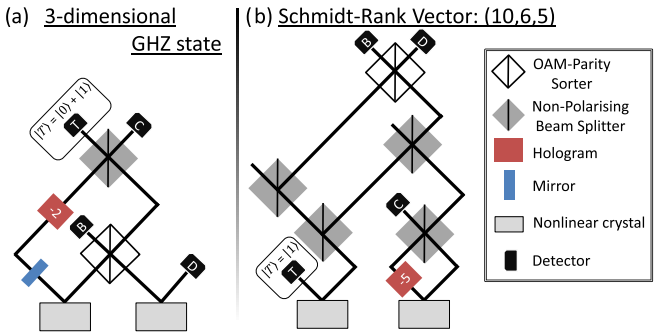


FIG. 2. Experimental implementations of high-dimensional multipartite entangled quantum states. (a) The experimental implementation for a three-dimensional three-partite GHZ state. If detector $T$ (Trigger) observes a photon in the state $|T\rangle = (|0\rangle + |1\rangle)$, then the rest of the quantum state is in a GHZ state, which looks like $|\psi\rangle = |0,0,0\rangle + |1,1,1\rangle + |2,2,2\rangle$ (up to local transformations). The parity sorter, as described in [37], can sort even and odd OAM modes. The three-dimensional GHZ state has a Schmidt-rank vector of (3,3,3) (all components are symmetrically entangled with the rest of the state). (b) A more complex experiment is required for higher-order Schmidt-rank vectors. The (10,6,5) state is one example of asymmetrically entangled quantum states. The experiments are just two examples of 51 implementations found for creating a variety of different entangled states.

One arm is used to trigger the tripartite state in the other three arms, which leads to roughly $10^{15}$ possible configurations. At the end, a postselection procedure consisting of the coincidence detection of four photons in the first four arms yields the final state.

We calculate the Schmidt-rank vector of the final state and select nontrivial ones (i.e., where there are no separable parties). Furthermore, for higher usefulness in experiments, we demand that the final state is maximally entangled in its orbital-angular-momentum. If the criteria hold, the experiment is reported.

MELVIN runs for roughly 150 hours (on an Intel Core i7 notebook with 2,4 GHz and 24 GB RAM using Wolfram Mathematica), and finds 51 experiments for states that are entangled in genuinely different ways. Among them, we find the first experimentally realizable scheme of a high-dimensional GHZ state [10], a generalization of the well-studied two-dimensional GHZ state [Fig. 2(a)]. Furthermore, we find many experiments for different asymmetrically entangled states (such as the $|\psi_{4,2,2}\rangle$ discussed above). In addition, several experiments only differ by continuously tunable components (e.g., different holograms or triggers), making it possible to explore continuous transitions between states of different classes of entanglement.

The resulting experiments contain interesting novel experimental techniques previously unknown to the authors. For example, in 50 out of 51 experiments, one of the four paths that comes directly from the crystals has not been mixed with any other arm [arm $D$ in Fig. 2(a), and arm $T$ in 2(b)]. The reason is that, for double SPDC events, it is possible that the two photon pairs come from the same crystal. Leaving one path unmixed leads to erasure of such double-pair emission events in fourfold coincidence detection. Interestingly, this immediately introduces asymmetry in the final experimental configuration. A different novelty is introduced when more than six-dimensional entanglement is created beginning from two three-dimensional entangled pairs. This is only possible when the OAM spectra in two crystals are shifted with a hologram and combined in a nontrivial way [a preliminary stage of the technique can be seen in Fig. 2(b), where the spectrum in arm $C$ is shifted in order to reach a ten-dimensional output]. In other experiments, the normalization of the state has to be adjusted in order to get a maximally entangled output. As neutral-density filters were not part of the toolbox, MELVIN, instead, used beam splitters as a 50% filter [for example, Fig. 2(b)].

Now, we briefly explain the three-dimensional GHZ-state experiment [Fig. 2(a), details in [27] ]: Two independent SPDC events in two crystals (which produce three-dimensional entangled pairs) allow for nine different states in the four arms. The parity sorter effectively removes all combinations with opposite OAM parity from two crystals (such as $|0,0,-1,+1\rangle$), which reduces the state to five terms. Detection photon $T$ in the trigger state $|T\rangle = (|0\rangle + |1\rangle)$ leads to a multipartite entangled state where photons $C$ and $D$ reside in a three-dimensional space and photon $B$ lives in a two-dimensional space [17]. The dimensionality of photon $B$ is then increased from two to three in an intricate combination of photons $A$ and $C$. Photon $A$ is shifted by $-2$ OAM quanta and combined with photon $C$ at a beam splitter. These photons are then detected in the same mode in one BS output, which effectively erases the "which-crystal" information and entangles the remaining three photons into a three-dimensional GHZ state.

*Example 2: High-dimensional cyclic operations and learning.*—In the second example, we are interested in high-dimensional cyclic rotations, which are special cases of high-dimensional unitary transformations. A set of states is transformed in such a way that the last element of the set transforms to the first element (for example, $|1\rangle \to |2\rangle \to |3\rangle \to |1\rangle$ is a three cycle). Such transformations are required in novel kinds of high-dimensional quantum information protocols [38,39] as well as in the creation of high-dimensional Bell states. Here, our input is a set of high-dimensional states encoded in different degrees of freedom (path, polarization, and OAM). While the creation and verification of high-dimensional entanglement in OAM is well known [35,36], the knowledge of how to perform arbitrary transformations in this degree of freedom is still lacking. Thus, finding such transformations in OAM is very important, as it would enable practical experiments with high-dimensional

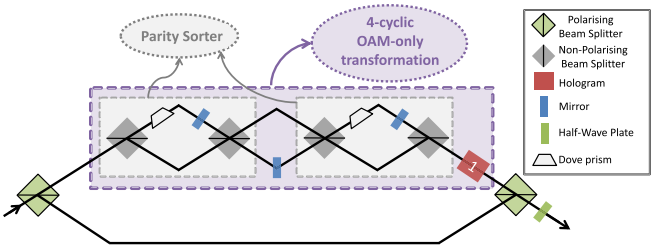


FIG. 3. Realization of an eight-cyclic rotation using polarization and OAM ($|-1,H\rangle \rightarrow |-1,V\rangle \rightarrow |0,V\rangle \rightarrow \cdots |2,H\rangle \rightarrow |-1,V\rangle$). In the experiment, a four-cyclic rotation for pure OAM values is used. Within the four-cyclic rotation, the parity sorter [37] mentioned in the main text is used twice.

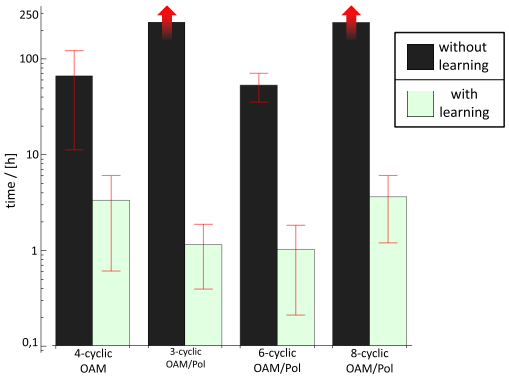


FIG. 4. Comparison of performance with and without the ability to learn (log scale). White shows the average time required in the case where the algorithm can learn useful transformations (the algorithm was executed 10 times with the same initial conditions). Black shows the time it requires without the ability to learn. The experiments for three-cyclic and eight-cyclic transformations were not found (within 250 hours) without learning, while experiments for four-cyclic and six-cyclic rotation were found three and four times in 250 hours, respectively. The errors stand for 1 standard deviation, calculated from the times it took to find the solution. Thus, autonomously extending the set of useful transformations improves MELVIN's performance, which is crucial for scaling to more complex experiments.

quantum states and find application in high-dimensional quantum information protocols.

The experiments are generated using a set of basic elements that consists of polarizing and nonpolarizing beam splitters, Dove prisms, mirrors, holograms, and half-wave plates. These elements are placed in one of three different paths (one path is used as an input, and two empty paths are added to increase variability). This leads to roughly $10^{22}$ different possible experimental configurations.

The criterion is based on the largest cycle of the transformation: A number of input states [with different polarization (horizontal and vertical), OAM ($\ell = -10$ to $+10$) and paths] are calculated. Then, we search subsets of modes that are transformed in a closed cycle, as described above, and select the largest closed cycle. MELVIN was able to find the first experimentally realizable OAM-only four-cyclic transformation, OAM-polarization hybrid three-, six-, and eight-cyclic rotations and up to 14-cyclic rotations using OAM, polarization, and path (Fig. 3 and [27]).

Complex problems can be solved more efficiently by reusing solutions to simpler problems [40,41]: Whenever MELVIN finds a solution for a simpler system, it memorizes the experimental configuration as a new part of its initial toolbox [27]. The novel elements in the toolbox can be used to construct the next experimental configuration. To compare the effectiveness of learning, we analyze the algorithm with and without the ability to increase its own set of basic elements. We ran the algorithm for 250 hours, and only three and four instances of four-cyclic and six-cyclic rotations were found, respectively. Not a single instance of a three-cyclic or an eight-cyclic rotation was found within 250 hours. However, using the ability to learn new elements, we ran the algorithm 10 times (starting with the initial toolbox, i.e., without keeping the learned elements), and discovered that the three- and six-cyclic rotations were found, on average, within 90 minutes (they were always found within three hours), and the four- and eight-cyclic rotations were found, on average, within three to five hours (in each of the ten trials, they were found within eight hours). Thus, the ability to learn new elements improves the search by more than 1 order of magnitude, suggesting a mechanism for designing experiments with a higher complexity (Fig. 4).

*Conclusion and outlook.*—We have shown how a computer can find new quantum experiments. The large number of discoveries reveals a way to investigate new families of complex entangled quantum systems in the laboratory. Several of these experiments are being built at the moment in our labs [17,18]. In contrast to human designers of experiments, MELVIN does not follow intuitive reasoning about the physical system and, therefore, leads to the utilization of many unfamiliar and unconventional techniques that are challenging to understand. The algorithm can learn from experience (i.e., previous successful solutions), which leads to a significant speed-up in discoveries of more complex experiments.

MELVIN can be applied to many other questions about the creation and manipulation of quantum systems, such as the search for more general high-dimensional transformations with different degrees of freedom and for different physical systems such as ultracold atoms [28] or for efficient generation of other types of important quantum systems such as NOON states [19]. In order to improve the efficiency of finding solutions, powerful techniques from artificial intelligence research can be applied, such as evolutionary algorithms [42] (where the experiment and the resulting quantum state play the role of genotype and phenotype, respectively), reinforcement learning techniques [41,43,44] (by implementing a reward function depending on the closeness of the quantum states properties to the desired properties), or

entropy-based [45] and big-data methods [46] (in order to find more unexpected solutions).

We thank Daniel Greenberger, Marcus Huber, Hans Briegel, Nora Tischler, and Dominik Leitner for fruitful discussions and/or critical reading of our manuscript. This project was supported by the Austrian Academy of Sciences (ÖAW), the European Research Council (SIQS Grant No. 600645 EU-FP7-ICT), the Austrian Science Fund (FWF) with SFB F40 (FOQUS). M. M. acknowledges support from the European Commission through a Marie Curie Fellowship (OAMGHZ).

*mario.krenn@univie.ac.at
†Present address: Department of Physics and Max Planck Centre for Extreme and Quantum Photonics, University of Ottawa, Ottawa K1N 6N5, Canada.
‡Present address: Faculty of Physics, University of Warsaw, Pasteura 5, 02-093 Warsaw, Poland.

[1] C. H. Bennett, G. Brassard, C. Crépeau, R. Jozsa, A. Peres, and W. K. Wootters, Phys. Rev. Lett. **70**, 1895 (1993).
[2] X.-L. Wang, X.-D. Cai, Z.-E. Su, M.-C. Chen, D. Wu, L. Li, N.-L. Liu, C.-Y. Lu, and J.-W. Pan, Nature (London) **518**, 516 (2015).
[3] C. K. Hong, Z. Y. Ou, and L. Mandel, Phys. Rev. Lett. **59**, 2044 (1987).
[4] M. O. Scully and K. Drühl, Phys. Rev. A **25**, 2208 (1982).
[5] E. Schrödinger, Naturwissenschaften **23**, 823 (1935).
[6] A. Einstein, B. Podolsky, and N. Rosen, Phys. Rev. **47**, 777 (1935).
[7] J. S. Bell, Physics (Long Island City, N.Y.) **1**, 195 (1964).
[8] D. M. Greenberger, M. A. Horne, and A. Zeilinger, in *Bells Theorem, Quantum Theory and Conceptions of the Universe* (Springer, New York, 1989), pp. 69–72.
[9] M. Huber and J. I. de Vicente, Phys. Rev. Lett. **110**, 030501 (2013).
[10] J. Lawrence, Phys. Rev. A **89**, 012105 (2014).
[11] A. K. Ekert, Phys. Rev. Lett. **67**, 661 (1991).
[12] U. Vazirani and T. Vidick, Phys. Rev. Lett. **113**, 140501 (2014).
[13] P. W. Shor, in *35th Annual Symposium on Foundations of Computer Science: proceedings; 1994, Santa Fe, New Mexico* (IEEE, New York, 1994), pp. 124–134.
[14] P. Rebentrost, M. Mohseni, and S. Lloyd, Phys. Rev. Lett. **113**, 130503 (2014).
[15] A. N. Boto, P. Kok, D. S. Abrams, S. L. Braunstein, C. P. Williams, and J. P. Dowling, Phys. Rev. Lett. **85**, 2733 (2000).
[16] G. Tóth and I. Apellaniz, J. Phys. A **47**, 424006 (2014).
[17] M. Malik, M. Erhard, M. Huber, M. Krenn, R. Fickler, and A. Zeilinger, arXiv:1509.02561.
[18] F. Schlederer, M. Krenn, R. Fickler, M. Malik, and A. Zeilinger, arXiv:1512.02696.
[19] I. Afek, O. Ambar, and Y. Silberberg, Science **328**, 879 (2010).
[20] X. Y. Zou, L. J. Wang, and L. Mandel, Phys. Rev. Lett. **67**, 318 (1991).
[21] G. B. Lemos, V. Borish, G. D. Cole, S. Ramelow, R. Lapkiewicz, and A. Zeilinger, Nature (London) **512**, 409 (2014).
[22] V. V. Shende, S. S. Bullock, and I. L. Markov, IEEE Trans. Comput.-Aided Des. Integr. Circuits Syst., **25**, 1000 (2006).
[23] D. Maslov, G. W. Dueck, D. M. Miller, and C. Negrevergne, IEEE Trans. Comput.-Aided Des. Integr. Circuits Syst. **27**, 436 (2008).
[24] M. Saeedi and I. L. Markov, ACM Comput. Surv. **45**, 21 (2013).
[25] A. Bocharov, M. Roetteler, and K. M. Svore, Phys. Rev. A **91**, 052317 (2015).
[26] A. Bocharov, M. Roetteler, and K. M. Svore, Phys. Rev. Lett. **114**, 080502 (2015).
[27] See Supplemental Material at http://link.aps.org/supplemental/10.1103/PhysRevLett.116.090405 for details of experimental toolbox, details to all designed experiments, detailed calculation of the 3-dimensional GHZ setup, and information about the experiment simplification.
[28] P. Wigley, P. Everitt, A. Hengel, J. Bastian, M. Sooriyabandara, G. McDonald, K. Hardman, C. Quinlivan, M. Perumbil, C. Kuhn *et al.*, arXiv:1507.04964.
[29] M. Huber, M. Perarnau-Llobet, and J. I. de Vicente, Phys. Rev. A **88**, 042328 (2013).
[30] J. Cadney, M. Huber, N. Linden, and A. Winter, Linear Algebra Appl. **452**, 153 (2014).
[31] D. Bouwmeester, J.-W. Pan, M. Daniell, H. Weinfurter, and A. Zeilinger, Phys. Rev. Lett. **82**, 1345 (1999).
[32] X.-C. Yao, T.-X. Wang, P. Xu, H. Lu, G.-S. Pan, X.-H. Bao, C.-Z. Peng, C.-Y. Lu, Y.-A. Chen, and J.-W. Pan, Nat. Photonics **6**, 225 (2012).
[33] L. Allen, M. W. Beijersbergen, R. J. C. Spreeuw, and J. P. Woerdman, Phys. Rev. A **45**, 8185 (1992).
[34] A. C. Dada, J. Leach, G. S. Buller, M. J. Padgett, and E. Andersson, Nat. Phys. **7**, 677 (2011).
[35] J. Romero, D. Giovannini, S. Franke-Arnold, S. M. Barnett, and M. J. Padgett, Phys. Rev. A **86**, 012334 (2012).
[36] M. Krenn, M. Huber, R. Fickler, R. Lapkiewicz, S. Ramelow, and A. Zeilinger, Proc. Natl. Acad. Sci. U.S.A. **111**, 6243 (2014).
[37] J. Leach, M. J. Padgett, S. M. Barnett, S. Franke-Arnold, and J. Courtial, Phys. Rev. Lett. **88**, 257901 (2002).
[38] M. Araújo, F. Costa, and Č. Brukner, Phys. Rev. Lett. **113**, 250402 (2014).
[39] A. Tavakoli, I. Herbauts, M. Żukowski, and M. Bourennane, Phys. Rev. A **92**, 030302 (2015).
[40] M. Schmidt and H. Lipson, Science **324**, 81 (2009).
[41] H. J. Briegel and G. De las Cuevas, Sci. Rep. **2**, 400 (2012).
[42] A. E. Eiben and J. Smith, Nature (London) **521**, 476 (2015).
[43] M. L. Littman, Nature (London) **521**, 445 (2015).
[44] V. Mnih, K. Kavukcuoglu, D. Silver, A. A. Rusu, J. Veness, M. G. Bellemare, A. Graves, M. Riedmiller, A. K. Fidjeland, G. Ostrovski *et al.*, Nature (London) **518**, 529 (2015).
[45] A. D. Wissner-Gross and C. E. Freer, Phys. Rev. Lett. **110**, 168702 (2013).
[46] L. R. Varshney, F. Pinel, K. R. Varshney, D. Bhattacharjya, A. Schoergendorfer, and Y.-M. Chee, arXiv:1311.1213.